nature chemical biology

ARTICLE

PUBLISHED ONLINE: 24 AUGUST 2015 | DOI: 10.1038/NCHEMBIO.1891

Human calprotectin is an iron-sequestering host-defense protein

Toshiki G Nakashige[1], Bo Zhang[2], Carsten Krebs[2,3] & Elizabeth M Nolan[1]*

Human calprotectin (CP) is a metal-chelating antimicrobial protein of the innate immune response. The current working model states that CP sequesters manganese and zinc from pathogens. We report the discovery that CP chelates iron and deprives bacteria of this essential nutrient. Elemental analysis of CP-treated growth medium establishes that CP reduces the concentrations of manganese, iron and zinc. Microbial growth studies reveal that iron depletion by CP contributes to the growth inhibition of bacterial pathogens. Biochemical investigations demonstrate that CP coordinates Fe(II) at an unusual hexahistidine motif, and the Mössbauer spectrum of ^{57}Fe(II)-bound CP is consistent with coordination of high-spin Fe(II) at this site (δ = 1.20 mm/s, ΔE_Q = 1.78 mm/s). In the presence of Ca(II), CP turns on its iron-sequestering function and exhibits subpicomolar affinity for Fe(II). Our findings expand the biological coordination chemistry of iron and support a previously unappreciated role for CP in mammalian iron homeostasis.

Transition metal ions are essential nutrients for all organisms[1]. In the vertebrate host, microbial pathogens must acquire first-row transition metal ions (including iron (Fe), manganese (Mn) and zinc (Zn)) to replicate, colonize and cause disease[2–6]. Metal-ion withholding is an accepted mechanism of immunity, often termed nutritional immunity[2,4], and a number of metal-chelating host-defense factors are used during the early stages of infection to prevent microbial acquisition of essential nutrient metals. In humans and other mammals, one of these factors is calprotectin, an oligomer of the calcium-binding proteins S100A8 (also called myeloid-related protein (MRP)-8 or calgranulin A) and S100A9 (also called MRP-14 or calgranulin B)[4,6–8]. Abundant in neutrophils and produced by epithelial cells, CP is released at sites of infection and has antimicrobial activity that is attributed to its ability to scavenge manganese and zinc[7–13].

CP is a member of the S100 protein family, and the human form exists as either a heterodimer ($\alpha\beta$) or heterotetramer ($\alpha_2\beta_2$) of S100A8 (α) and S100A9 (β)[14]. Each subunit contains two Ca(II)-binding EF-hand domains and two additional sites for transition metal ions form at the S100A8–S100A9 heterodimer interface (**Fig. 1** and **Supplementary Results**, **Supplementary Fig. 1**)[9–13,15,16]. Site 1 is a His_3Asp motif comprised of S100A8 residues His83 and His87 and S100A9 residues His20 and Asp30 (**Fig. 1b**). Site 1 binds Zn(II) with high affinity and has relatively weak affinity for Mn(II)[10,11]. Site 2 is an unusual histidine-rich site that was first identified as a tetrahistidine (His_4) motif comprising S100A8 residues His17 and His27 and S100A9 residues His91 and His95 (ref. 16). Subsequent structural[12,15] and spectroscopic[13,15] investigations of manganese-bound CP revealed that site 2 provides a remarkable hexahistidine (His_6) site for this metal ion with His103 and His105 of the S100A9 C-terminal tail completing an octahedral coordination sphere (**Fig. 1c**). Site 2 binds both Mn(II) and Zn(II) with high affinity and exhibits a thermodynamic preference for Zn(II)[11–13]. Moreover, site 2 is important for the antibacterial activity of CP against a variety of Gram-negative and Gram-positive strains[10,12,13]. Loss of site 2 (such as in the ΔHis_4 or AAA variant, **Supplementary Table 1**) is reported to be more detrimental to the antimicrobial activity of CP than the removal of site 1 (ΔHis_3Asp)[10,12,13]. Because site 2 is the high-affinity Mn(II) site, the broad-spectrum *in vitro* antimicrobial activity of CP has been attributed to Mn(II) deprivation[12]. Indeed, a significant body of recent work indicates that various human pathogens (such as *Staphylococcus aureus*, *Streptococcus pneumoniae* and *Borrelia burgdorferi*) must acquire manganese to be virulent[17–20]. A robust host-defense mechanism to prevent manganese acquisition is therefore important, and to date, CP is the only Mn(II)-sequestering protein that has been identified in humans[8]. Nevertheless, we questioned a generalized Mn(II)-centric model for site 2 and the antimicrobial activity of CP[13]. The specific metal-ion requirements vary amongst organisms, and some of the bacterial strains less susceptible to the site 2 variants have minimal metabolic requirements for manganese[10,12,13,21].

We therefore hypothesized that chelation of another as-yet unidentified first-row transition metal ion at site 2 occurs and contributes to the growth inhibitory activity of CP. This hypothesis is contrary to prior reports, which concluded that CP does not bind iron or copper[8,12,14]. The Irving-Williams series[22], a tenet of coordination chemistry, describes the relative affinities of a given chelator for divalent first-row transition metal ions (manganese < iron < cobalt < nickel < copper > zinc). Although first defined for small-molecule octahedral metal complexes, this series is often employed to rationalize the relative divalent metal-ion affinities of metalloproteins. The relative Mn(II) and Zn(II) affinities of each CP site ($K_{d,Mn} > K_{d,Zn}$) follow this trend[10,11,23], and we expected the nitrogen-rich metal-chelating motifs to coordinate first-row transition metals that lie between manganese and zinc in the periodic table.

To test our hypothesis, we first employed an unbiased approach to evaluate which metal ions CP sequesters in the context of microbial growth assays. On the basis of these initial studies and subsequent investigations, we uncovered a new dimension of the biological coordination chemistry and growth inhibitory function of CP. Contrary to current understanding, we discovered that CP sequesters iron. Our findings afford a new model for the antimicrobial action of CP and indicate a heretofore-unrecognized role for CP in mammalian iron homeostasis. Moreover, biochemical and spectroscopic investigations of CP reveal high-affinity coordination of ferrous iron at a binding site unique amongst known iron-containing proteins and thereby expand the biological coordination chemistry of Fe(II).

[1]Department of Chemistry, Massachusetts Institute of Technology, Cambridge, Massachusetts, USA. [2]Department of Chemistry, Pennsylvania State University, University Park, Pennsylvania, USA. [3]Department of Biochemistry and Molecular Biology, Pennsylvania State University, University Park, Pennsylvania, USA. *e-mail: lnolan@mit.edu

RESULTS

CP depletes iron from bacterial growth medium

To evaluate the metal sequestration properties of CP, we performed a series of metal-ion depletion experiments (**Fig. 2**, **Supplementary Tables 2–10** and **Supplementary Figs. 2** and **3**). We treated a standard growth medium employed in antimicrobial activity assays with the CP-Ser variant (S100A8^{C42S}–S100A9^{C3S})—which we routinely employ in metal-binding studies and that exhibits comparable antibacterial activity to native CP[10]—or a metal-binding site variant, in which select metal-chelating residues were replaced by alanines (**Supplementary Table 1**). We then quantified the amounts of residual manganese, iron, cobalt, nickel, copper and zinc in the medium with or without CP-Ser or variant treatment using inductively coupled plasma (ICP) mass spectrometry (ICP-MS) or ICP–optical emission spectroscopy (ICP-OES). The CP-Ser ΔHis_3Asp and ΔHis_4 variants are deletion mutants of the His_3Asp and His_4 binding sites, respectively. We define the His_4 site as the four histidine residues of site 2 that reside at the S100A8–S100A9 interface (**Fig. 1** and **Supplementary Table 1**). The AAA variant lacks three histidine residues at positions 103–105 of the S100A9 C-terminal tail, and the ΔΔ variant has neither the His_3Asp nor the His_4 site. Because the Mn(II) and Zn(II) affinities of CP, as well as its antimicrobial activity, are enhanced in the presence of excess Ca(II)[10,11], we prepared samples of the medium with (+Ca(II)) or without (−Ca(II)) a 2-mM Ca(II) supplement. We also reported that β-mercaptoethanol (BME) enhances the antimicrobial activity of both native CP and CP-Ser[10] and therefore evaluated the effect of this reducing agent on metal depletion. The tryptic soy broth (TSB)–Tris buffer growth medium used in these studies is routinely employed for evaluating the antimicrobial activity of CP and contains ~150 nM manganese, ~3 μM iron and ~5 μM zinc (**Supplementary Table 2**). The manganese concentration decreased by a factor of 3.7 (−Ca(II), +BME) or 6.9 (+Ca(II), +BME) (**Fig. 2a**), and the zinc concentration decreased by a factor of 48 (−Ca(II), +BME) or 59 (+Ca(II), +BME) (**Fig. 2b**) when the medium was treated with 250 μg/ml of CP. The relative manganese and zinc levels obtained for medium treated with the CP mutants were consistent with two central conclusions from prior Mn(II)- and Zn(II)-binding studies: (i) CP binds Zn(II) with high affinity at both sites 1 and 2 and (ii) CP binds Mn(II) with high affinity only at site 2 (refs. 10–12).

CP treatment also resulted in depletion of other first-row transition metals in the growth medium (**Supplementary Tables 2–10** and **Supplementary Fig. 2**), consistent with our reasoning that one or both of the interfacial sites accommodate such metals. Most notably, the addition of 250 μg/ml of CP to the medium caused iron levels to decrease by a factor of 3.5 (−Ca(II), +BME) or 23 (+Ca(II), +BME) (**Fig. 2c**). The Ca(II) dependence indicated that CP binds iron more tightly in the presence of Ca(II), in agreement with our prior studies of Mn(II)[11] and Zn(II)[10] sequestration. The 23-fold decrease in iron under '+Ca(II), +BME' conditions reduced its concentration in the growth medium to ~80 nM. Moreover, maximal iron depletion occurred in the presence of excess BME, suggesting a role of the redox environment for this metal. The relative iron concentrations obtained following treatment of the medium with the CP variants indicated that the His_6, and not the His_3Asp, site was essential for iron depletion. In total, this analysis revealed that CP removes iron from the growth medium and supported a new hypothesis in which iron deprivation contributes to the antimicrobial activity of CP.

Iron depletion contributes to bacterial growth inhibition

To examine the effect of metal depletion on bacterial growth by CP, we employed CP-treated medium and tested a panel of Gram-negative and Gram-positive bacterial strains, all of which have a metabolic iron requirement, in growth assays (**Fig. 3** and **Supplementary Figs. 4** and **5**). We supplemented the CP-treated medium with manganese, iron and/or zinc, in all possible combinations, to achieve the metal concentrations of the untreated medium and monitored bacterial growth over a 20-h period. In all cases, maximum growth recovery occurred only when the metal supplement contained iron. This phenomenon was most striking for the Gram-negative organisms, for which iron supplementation alone was necessary and sufficient to restore full growth, but was also the case for the Gram-positive strains where both manganese and iron were required to achieve maximum growth recovery.

In a second series of growth studies, we performed antimicrobial activity assays using *Escherichia coli* and *S. aureus* and compared the growth inhibitory activities of CP-Ser, ΔHis_3Asp and ΔHis_4. These proteins were preincubated with 0.9 equiv of iron supplied as an Fe(II) salt (**Fig. 4a**,**b**). Preincubation with iron attenuated the antimicrobial activity of CP to levels comparable to that of ΔHis_4 and completely blocked the activity of ΔHis_3Asp against both species. These experiments further supported the importance of site 2 in the antibacterial activity of CP against these two organisms and showed that addition of Fe(II) blocks the activity associated with this site.

In a third series of growth studies, we treated *Lactobacillus plantarum* with CP-Ser, ΔHis_3Asp, ΔHis_4 or the AAA variant (**Fig. 4c**,**d** and **Supplementary Fig. 6**). Unlike the organisms described previously, *L. plantarum* has no metabolic iron requirement[24]. The lactobacilli growth medium employed in our experiments is rich in manganese (~100 μM, **Supplementary Table 11**), and full growth inhibition was observed (+Ca(II), ± BME) with 500 μg/ml (~20 μM) of CP-Ser, ΔHis_4 and AAA. In contrast, the antimicrobial activity was completely attenuated for ΔHis_3Asp. The lactobacilli growth medium contains ~10 μM zinc, and we attribute the growth inhibitory function of CP against *L. plantarum* to Zn(II) sequestration by the His_3Asp site (**Fig. 4e** and **Supplementary Tables 12** and **13**). In total, these metal depletion and growth studies revealed that: (i) site 2 binds multiple metals such that the antimicrobial activity associated with site 2 cannot be attributed only to manganese chelation, (ii) CP sequesters iron, and iron depletion inhibits the growth of both Gram-negative and Gram-positive organisms and (iii) the site dependence will be determined by the metal requirements of a given organism as well as the availability of the metal ion.

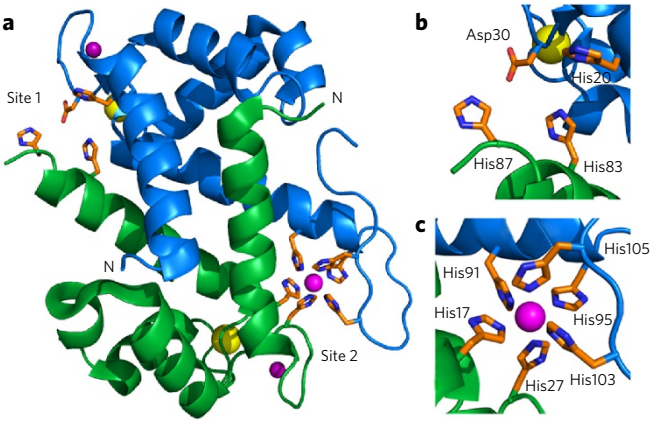

Figure 1 | CP houses two transition metal–binding sites at the S100A8–S100A9 interface. (**a**) CP heterodimer from the structure of the Mn(II)-, Ca(II)- and Na(I)-bound heterotetramer (PDB: 4XJK)[15]. S100A8 is shown in green and S100A9 in blue. The calcium ions are shown as yellow spheres. The sodium ions are shown as purple spheres. The manganese ion is shown as a magenta sphere. The residues at the metal-binding sites are shown as orange sticks. (**b**) The His_3Asp motif (site 1) is comprised of S100A8 residues His83 and His87 and S100A9 residues His20 and Asp30. (**c**) The His_6 motif (site 2) is comprised of S100A8 residues His17 and His27 and S100A9 residues His91, His95, His103 and His105.

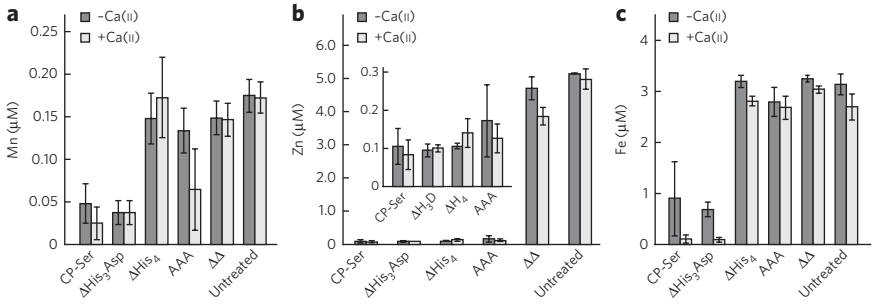

Figure 2 | CP depletes metals from bacterial growth medium. (**a**–**c**) Metal analysis of manganese (Mn, **a**), zinc (Zn, **b**) and iron (Fe, **c**) concentrations in CP-treated and untreated growth medium (250 μg/ml CP, ~3 mM BME) in the absence (light gray bars) or presence (dark gray bars) of a 2-mM Ca(II) supplement (data are mean ± s.e.m., n = 7 for untreated samples, n = 4 for CP-Ser–treated samples, n = 3 for all other samples).

CP blocks bacterial iron uptake

In a fourth series of growth studies, we examined uptake of the radioactive isotope ^{55}Fe by *E. coli* and *Pseudomonas aeruginosa* in the absence or presence of CP or the ΔΔ variant (**Fig. 5**). This experiment was initiated by transferring bacteria cultured in a minimal medium to an uptake assay medium containing ~3 mM BME, ~2 mM Ca(II) and ~3 μM $FeCl_3$ (1:9 ratio of ^{55}Fe:unlabeled Fe) with or without 500 μg/ml CP-Ser or the ΔΔ variant. These experiments employed a higher inoculum (OD_{600} = 0.2) than that used for antibacterial activity assays (OD_{600} ~0.001; **Fig. 4a** and **Supplementary Fig. 7**), and 500 μg/ml CP was not sufficient to inhibit bacterial growth at this cell density. Over the course of a 2-h growth period in the uptake medium, the OD_{600} of the cultures increased from ~0.2 to either ~0.6 (*E. coli*) or ~0.4 (*P. aeruginosa*) and was unaffected by the presence of CP-Ser or the ΔΔ variant (**Fig. 5**, lower panels). Quantification of ^{55}Fe uptake over time indicated that the presence of 500 μg/ml CP-Ser in the medium reduced bacterial ^{55}Fe uptake by two- to three-fold relative to that in the untreated or ΔΔ-treated cultures following a 2-h incubation (**Fig. 5**, upper panels). These results establish that supplementation of medium with CP-Ser can prevent microbial iron uptake and that this effect requires the metal-binding sites.

CP coordinates Fe(II) at the histidine-rich motif

Iron exists in several biologically accessible oxidation states[25]. We observed that either BME[10] or dithiothreitol (DTT) enhanced the antimicrobial activity of CP against *E. coli* and *S. aureus*, indicating that the effect is not specific to one reducing agent or microorganism (**Supplementary Fig. 8**). Taken together with the knowledge that CP sequesters iron, the BME-DTT effect provides circumstantial evidence that CP prefers to coordinate Fe(II) over Fe(III). To evaluate this notion, we preincubated CP-Ser with Fe(II) or Fe(III), performed analytical size-exclusion chromatography (SEC) and analyzed the fractions for CP-Ser and iron (**Fig. 6a**–**c**). We observed an SEC peak shift with the addition of Fe(II), but not Fe(III), and demonstrated that CP bound and retained Fe(II) during elution. The residues of the His_6 site, and not those of the His_3Asp motif, were required for the Fe(II)-induced peak shift (**Fig. 6d**–**f** and **Supplementary Figs. 9**–**11**). These observations provided compelling evidence for Fe(II) complexation at the His_6 site and are analogous to the trends we observed for Mn(II) in prior work[13].

In addition, we employed Mössbauer spectroscopy to confirm Fe(II) coordination by CP at the His_6 site. The 4.2-K/53-mT Mössbauer spectrum of CP-Ser in the presence of a substoichiometric amount of ^{57}Fe(II) sulfate (**Fig. 6g**, vertical bars) displays a broad quadrupole doublet. The spectrum is markedly different from that of ^{57}Fe(II) sulfate in buffer (**Fig. 6g**, orange line), demonstrating that Fe(II) is binding to CP-Ser. Moreover, the Mössbauer spectra of ^{57}Fe(II)-bound CP-Ser and ^{57}Fe(II)-bound ΔHis_3Asp (**Supplementary Fig. 12**) are essentially indistinguishable, which strongly suggests that Fe(II) is coordinated at the His_6 site. The spectrum can be simulated either as a single quadrupole doublet with an isomer shift (δ) of 1.20 mm/s and a quadrupole splitting parameter (ΔE_Q) of 1.78 mm/s (**Fig. 6g**, blue line) or as two quadrupole doublets (δ_1 = 1.18 mm/s, $\Delta E_{Q,1}$ = 1.68 mm/s (87%) and δ_2 = 1.21 mm/s, $\Delta E_{Q,2}$ = 2.32 mm/s (13%)). The latter analysis is supported by the 160-K spectrum, in which the resolution of the two components is enhanced (**Supplementary Fig. 13**). The large isomer shift value of 1.20 mm/s allows unambiguous assignment of the ^{57}Fe species as high-spin Fe(II) and is consistent with octahedral coordination of Fe(II) by the proposed His_6 site (**Supplementary Fig. 14**). Although the magnitude of ΔE_Q is smaller than those typically observed for high-spin Fe(II) complexes[26], smaller values of ΔE_Q are well documented for high-spin Fe(II) complexes[27–29].

CP binds Fe(II) with unprecedented high affinity

To participate in metal sequestration, CP must chelate the metal with high affinity, and its coordination sphere(s) must disfavor dissociation of the metal. Ferrous iron is a labile $3d^6$ metal ion, and the few reported Fe(II) affinities for metalloproteins and transcription factors are typically low (such as a K_d ~ 10^{-6}–10^{-5} M, ref. 30). To probe the Fe(II) affinity of CP, we performed Fe(II) competitions with CP and the Ca(II)-insensitive metal-ion sensor ZP1 (ref. 31). Titration of ZP1 with Fe(II) under anaerobic conditions resulted in

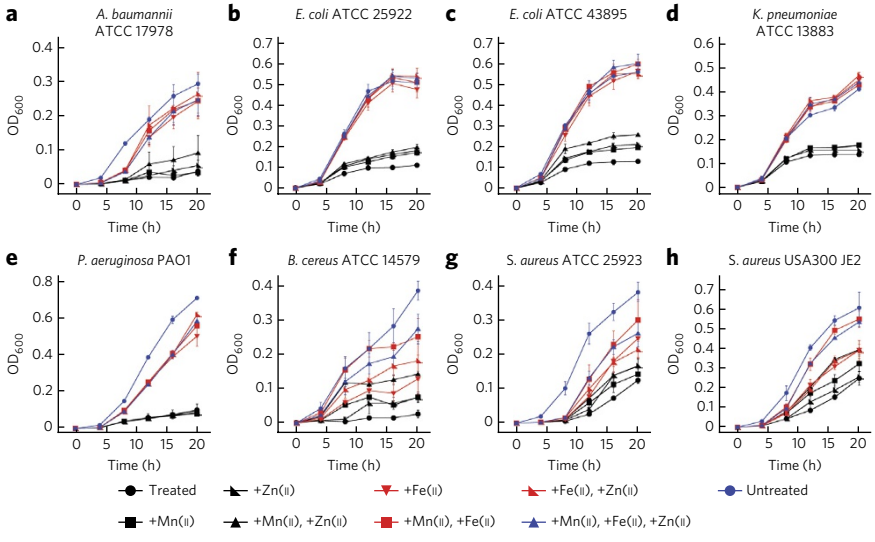

Figure 3 | Metal supplementation growth studies. (**a**–**h**) Growth curves of Gram-negative bacteria *Acinetobacter baumannii* (**a**), laboratory (**b**) and enterohemorrhagic (**c**) strains of *E. coli*, *Klebsiella pneumoniae* (**d**) and *P. aeruginosa* (**e**) and those of Gram-positive *Bacillus cereus* (**f**) and *S. aureus* (**g**,**h**) cultured in Ca(II)-containing medium (+BME) treated with CP-Ser (250 μg/ml) and supplemented with 0.15 μM Mn(II), 3 μM Fe(II) and/or 5 μM Zn(II). In all panels, data are mean ± s.e.m., n = 3 per group.

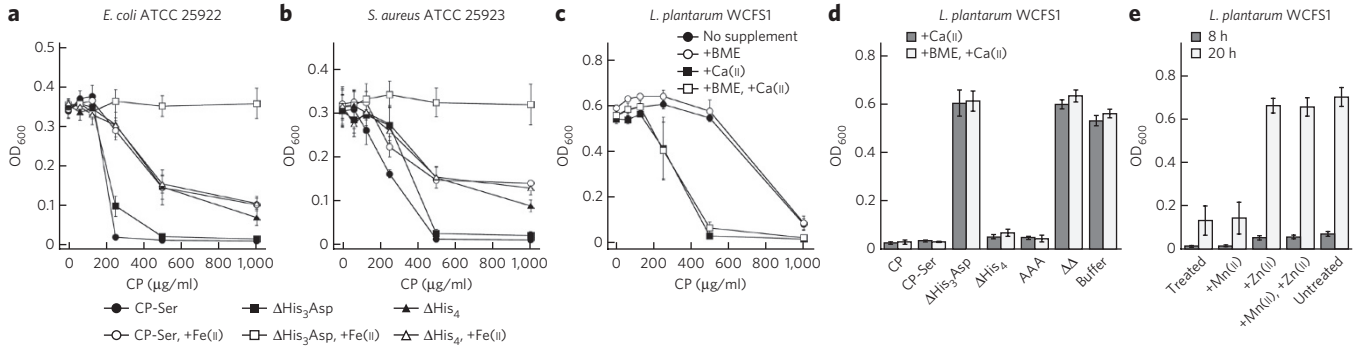

Figure 4 | The antimicrobial activity of CP against *E. coli*, *S. aureus* and *L. plantarum*. (**a**,**b**) Antibacterial activity of CP-Ser, ΔHis_3Asp and ΔHis_4 (apo or preincubated with 0.9 equiv of Fe(II)) against *E. coli* (**a**) and *S. aureus* (**b**) (t = 20 h; n = 6 per group). (**c**,**d**) Antibacterial activity of CP-Ser (**c**) or its variants (**d**) against *L. plantarum* in the absence or presence of 2-mM Ca(II) and 3-mM BME supplements (t = 20 h; n = 3 per group). In **d**, the protein concentration is 1.0 mg/ml. (**e**) Growth of *L. plantarum* in medium treated with CP-Ser (500 μg/ml) and supplemented with 10 μM Mn(II) and/or 10 μM Zn(II) (n = 3 per group). In all panels, data are mean ± s.e.m.

fluorescence quenching (**Supplementary Fig. 15**), as expected from prior investigations[31]. We determined the Fe(II) affinity of ZP1 by using buffers with fixed concentrations of free Fe(II) that spanned the 10^{-7} to 10^{-16} M range (**Supplementary Table 14**, **Supplementary Fig. 16** and **Supplementary Note**). These experiments provided a $K_{d1,Fe(II)}$ = 2.2 ± 0.3 pM for ZP1 at pH 7.0. Addition of Fe(II) to mixtures of ZP1 and CP-Ser in the absence of Ca(II) showed the same fluorescence response as a solution of ZP1 alone, which indicated that CP-Ser cannot compete with ZP1 for Fe(II) under low Ca(II) conditions (**Fig. 7b**,**c** and **Supplementary Note**). In contrast, native CP, CP-Ser and ΔHis_3Asp outcompeted ZP1 for Fe(II) binding in the presence of excess Ca(II) (**Fig. 7a**,**b**, **Supplementary Figs. 17–19** and **Supplementary Note**). Under these same high-Ca(II) conditions, negligible competition was observed for the ΔHis_4 and ΔΔ variants (**Fig. 7b**), and variable degrees of competition occurred for variants harboring mutations in the S100A9 C-terminal tail region (**Supplementary Fig. 20**).

To further examine the role of the S100A9 C-terminal tail region in Fe(II) coordination, we employed the colorimetric iron indicator ferrozine (a bidentate ligand that forms a 1:3 Fe(II):ferrozine complex ($K_{d,Fe(II)}$ = 3.0 × 10^{-16} M))[32] in competition assays with CP-Ser and five C-terminal tail variants (**Supplementary Table 1**, **Supplementary Fig. 21** and **Supplementary Note**). These assays were performed in the presence of 50 equiv of Ca(II). The $[Fe(II)ferrozine_3]^{2+}$ complex exhibits an absorbance feature at 562 nm (27,900 M^{-1} cm^{-1}) (ref. 33) and addition of 10 μM CP-Ser or the H104A variant to a solution containing 8 μM Fe(II) and 300 μM ferrozine resulted in a time-dependent loss of the optical absorption band for $[Fe(II)ferrozine_3]^{2+}$ over the course of 7 d. The absorption feature at 562 nm appeared with the subsequent addition of 10 μM Fe(II) (data not shown), which confirmed that the ability of ferrozine to detect Fe(II) was not compromised during the experiment. These results show that both CP-Ser and the H104A variant sequestered Fe(II) from ferrozine. Amino acid substitutions in the S100A9 C-terminal tail region resulted in attenuated competition. The AAA and AHA (comprising H103A and H105A) variants were unable to sequester Fe(II) from ferrozine, and the single variants H103A or H105A showed an intermediate behavior (**Supplementary Fig. 21**). This set of ferrozine competition assays, combined with the ZP1 competition assays (**Supplementary Fig. 20**), confirms that H103 and H105 in the S100A9 C-terminal tail region are essential for Fe(II) sequestration.

Other human S100 proteins, including S100A12, S100A7 and S100B, participate in the homeostasis of transition metal ions and form homodimers that display sites for transition metal binding at the dimer interface[23,34–36]. Because CP is the only S100 family member to exhibit a His_6 site, we reasoned that other S100 proteins are unable to bind Fe(II) with high affinity. Indeed, the ability of CP to outcompete picomolar-affinity ZP1 for Fe(II) was unique amongst the five human S100 proteins evaluated (**Supplementary Fig. 22** and **Supplementary Note**). This result is consistent with our prior study of Mn(II) sequestration, in which CP was the only S100 protein observed to sequester Mn(II) from ZP1 (ref. 13).

Taken together, the ZP1 and ferrozine competition assays: (i) confirmed that Ca(II) ions modulate the Fe(II) affinity of CP, (ii) revealed that CP houses a remarkably high-affinity Fe(II) site (consistent with its metal-sequestering function), (iii) implicated His103 and His105 of the S100A9 tail region in Fe(II) complexation and (iv) established that the Fe(II)-sequestering ability of CP is unique amongst human S100 proteins that form metal-binding sites at dimer interfaces.

Metal selectivity agrees with the Irving-Williams series

CP binds various first-row transition metal ions with high affinity, consistent with its metal-sequestering contribution to the innate immune response[9–13]. Taken together, reports of its Mn(II)- and Zn(II)-binding properties indicate that site 2 coordinates Mn(II) with K_d < 10 nM and Zn(II) with K_d < 240 pM (refs. 9–12,23). In agreement with expectations based on the Irving-Williams series (see above), CP has a thermodynamic preference for Zn(II) over Co(II) and Mn(II)[10,11]. On the basis of the Irving-Williams series and the

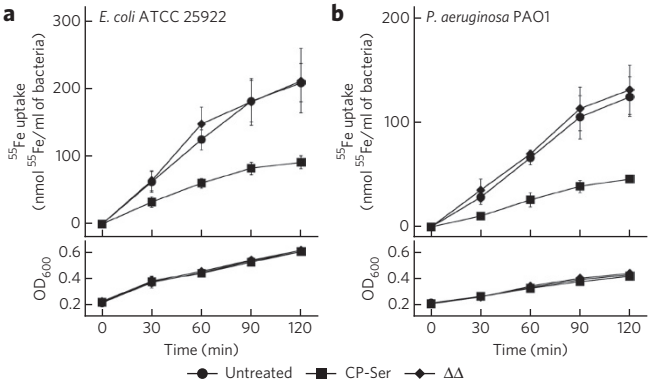

Figure 5 | Inhibition of bacterial iron acquisition by CP. Uptake of radiolabeled ^{55}Fe by *E. coli* (**a**) and *P. aeruginosa* (**b**) treated with either 500 μg/ml CP-Ser (squares) or ΔΔ (diamonds) or left untreated (circles). The upper panels show the amount of ^{55}Fe uptake per ml of bacterial culture over the 2-h experiment. The lower panels indicate the corresponding OD_{600} values of the cultures at each time point. The mean ± s.e.m. values for ^{55}Fe and OD_{600} are shown (n = 4 per group).

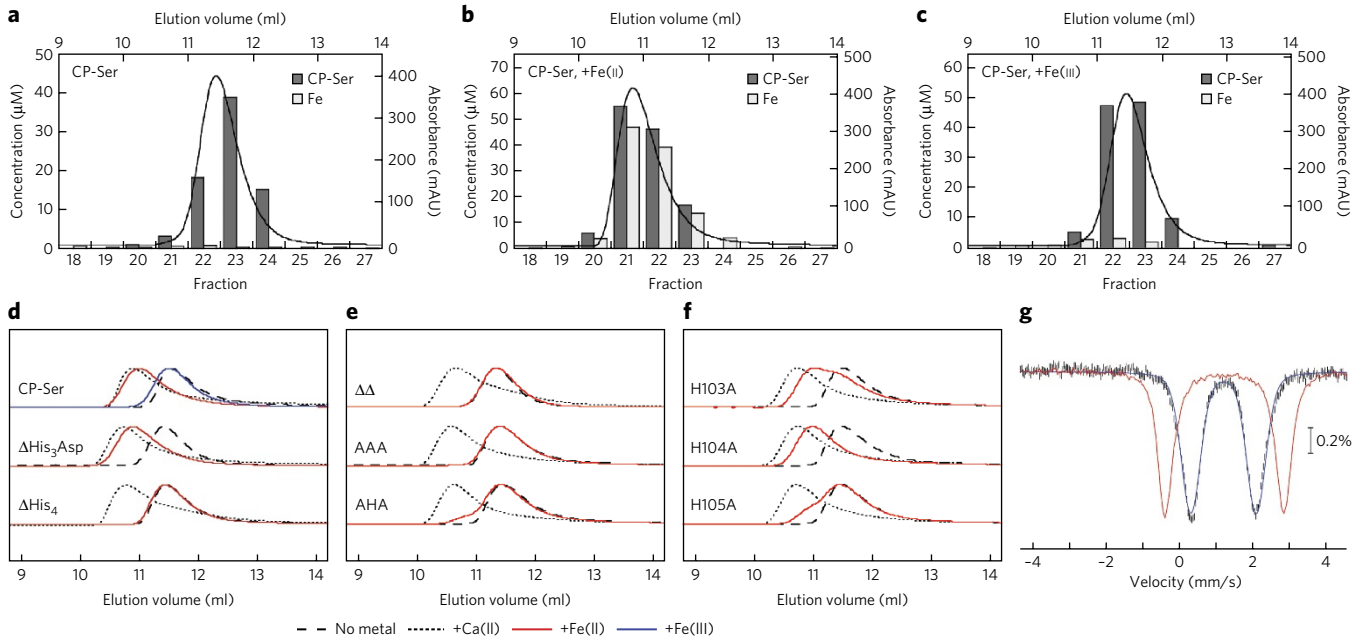

Figure 6 | Hexahistidine Fe(II) coordination by CP. (**a**–**c**) Analytical SEC chromatograms and quantification of iron and CP in eluent fractions of CP-Ser (400 μM) incubated with either no metal (**a**), 5 equiv of Fe(II) (**b**) or 5 equiv of Fe(III) (**c**). (**d**–**f**) Analytical SEC chromatograms of CP variants (20 μM) incubated with 10 equiv of Fe(II). Chromatograms for CP αβ (no metal) and $\alpha_2\beta_2$ (+Ca(II)) are provided for reference. Peak intensities are normalized to 1. (**g**) The 4.2-K/53-mT Mössbauer spectrum of ^{57}Fe(II)-bound CP-Ser (black vertical bar). Simulation using the parameters described in the main text is shown as the blue line, and the Mössbauer spectrum of Fe(II) sulfate in 50 mM Tris, pH 7.5 recorded under the same conditions is shown as the red line.

relative Mn(II)/Zn(II) and Co(II)/Zn(II) affinities of CP, we reasoned that CP will exhibit a thermodynamic preference for Fe(II) over Mn(II) and for Zn(II) over Fe(II). A series of metal substitution experiments, performed with or without excess Ca(II), supported this notion (**Fig. 7c–e** and **Supplementary Fig. 23**).

First, we employed room-temperature electron paramagnetic resonance (EPR) spectroscopy to determine whether addition of 0.9 equiv of Fe(II) to a solution in which 25 μM CP-Ser had been preincubated with 0.9 equiv of Mn(II) and 50 equiv of Ca(II) results in metal substitution at site 2. Both Fe(II)- and Mn(II)-CP are EPR silent at room temperature, whereas unbound or 'free' Mn(II) in solution displays a six-line pattern centered at a magnetic field corresponding to a *g*-value of ~2.0. We allowed the Mn(II)-CP (+Ca(II)) samples with and without added Fe(II) to incubate at room temperature for 7 d and observed that addition of Fe(II) to Mn(II)-CP (+Ca(II)) resulted in a more intense free-Mn(II) signal relative to that in the Mn(II)-CP-only control (**Fig. 7c**). Quantification of the free-Mn(II) signal revealed that the unbound Mn(II) concentration increased ~5-fold to ~14 μM when Fe(II) was added to the sample (**Fig. 7d**). This analysis indicates that Fe(II) substituted ~60% of the Mn(II) that was originally bound to site 2 and that both Fe(II)- and Mn(II)-bound CP exist in solution at this time point. To further probe Mn(II) and Fe(II) selectivity, we designed a ferrozine assay to monitor changes in the concentration of unbound Fe(II) following addition of 0.9 equiv of Fe(II) to a solution in which ΔHis_3Asp was preincubated with 0.9 equiv of Mn(II) in the absence or presence of 50 equiv of Ca(II) (**Supplementary Fig. 23**). In agreement with the conclusions from the room-temperature EPR study, this experiment revealed a time-dependent decrease in unbound Fe(II) and, in the +Ca(II) condition, showed that ~30% of the Mn(II) was displaced following a 24-h incubation.

Next we extended the ferrozine assay to evaluate the consequences of adding either 0.9 or 3 equiv of Zn(II) to a solution of 25 μM ΔHis_3Asp preincubated with 0.9 equiv of Fe(II). In agreement with our expectations, we observed that incubation of Fe(II)-bound ΔHis_3Asp with Zn(II) resulted in a time-dependent increase in free Fe(II) in solution (**Fig. 7e**). We performed these experiments in the absence of Ca(II) or presence of excess Ca(II), which revealed that Zn(II) more rapidly substitutes for Fe(II) in site 2 when Ca(II) is omitted from the buffer. In total, these experiments demonstrate that the metal selectivity of site 2 agrees with the Irving-Williams series.

Furthermore, the ferrozine assays indicated that the kinetics of metal substitution depend on Ca(II) and that Ca(II)-bound CP effectively entraps various first-row transition metals at site 2 (**Fig. 7e** and **Supplementary Fig. 23**). Although site 2 has the expected thermodynamic preference for Zn(II), we contend that site 2 will be populated with various metals *in vivo* because it will effectively sequester the metal ion that binds first. We reason that this scenario occurs in the extracellular space, where Ca(II) concentrations are high. Thus, kinetics as well as metal-ion availability at a given biological site will contribute to CP speciation in the biological milieu.

DISCUSSION

Previous investigations addressing the role of CP in the metal-withholding component of the host innate immune response have evaluated its ability to scavenge bioavailable manganese and zinc[7–13,37]. In this work, motivated by the hypothesis that CP chelates other first-row transition metal ions, we first employed an unbiased approach to evaluate which metal ions are sequestered by CP in a standard bacterial growth medium. The results from our experiments showed that CP depletes iron from growth medium and blocks iron uptake, indicating that iron chelation can contribute to its antimicrobial activity against both Gram-negative and Gram-positive organisms. Furthermore, our biochemical and spectroscopic investigations demonstrated that CP captures Fe(II) at a biologically unprecedented hexahistidine coordination motif at the S100A8–S100A9 dimer interface.

Our current results contrast two recent reports that concluded that CP does not chelate iron[8,12]. The first study analyzed the ability of CP to deplete select divalent cations from a growth medium. A negligible change in iron concentration (reported as percentage

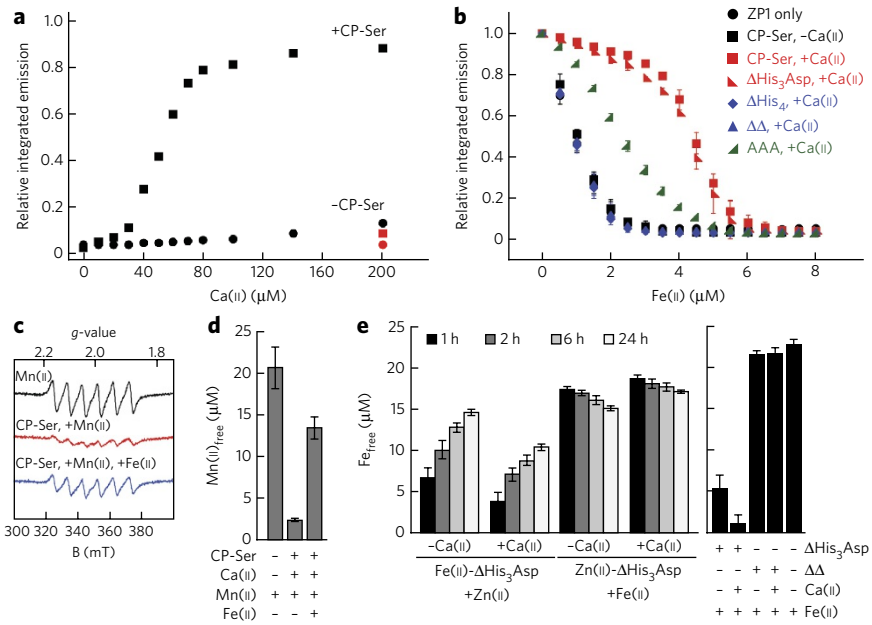

Figure 7 | CP binds Fe(II) with remarkably high affinity in a Ca(II)-dependent manner. (**a**) ZP1 (1 μM) emission response to 3.5 μM Fe(II) in the absence (circles) or presence (squares) of 4 μM CP-Ser with addition of Ca(II). The red markers represent samples containing 200 μM Ca(II), to which 4 μM Fe(II) was added at the end of the experiment (data represent the mean; $n = 2$). (**b**) ZP1 (1 μM) emission response to Fe(II) in the presence of 4 μM CP with or without 50 equiv of Ca(II) ($n = 3$ per group). (**c**) Room-temperature EPR spectra of Mn(II) (black), CP-Ser in the presence of 50 equiv of Ca(II) and 0.9 equiv of Mn(II) (red), and CP-Ser in the presence of 50 equiv of Ca(II) and 0.9 equiv of Mn(II) with the addition of 0.9 equiv of Fe(II) (blue). (**d**) The concentration of free Mn(II) as determined by room-temperature EPR ($n = 3$ per group). (**e**) The concentration of unbound Fe(II) in ΔHis_3Asp samples (containing 0.9 equiv of Fe(II)) after the addition of 0.9 equiv of Zn(II) ± 50 equiv of Ca(II) ($n = 3$ per group). Control samples containing 25 μM protein, 0.9 equiv of Fe(II) and/or 50 equiv of Ca(II) are shown in the right panel. In **b**,**d**,**e**, data are mean ± s.d.

of atoms in solution) was observed, whereas Mn(II) and Zn(II) levels were reduced[8]. In that experiment, the iron oxidation state and CP speciation were ambiguous. The second investigation reported an iron-binding titration assay, as monitored by isothermal titration calorimetry (ITC), in which CP-Ser was titrated with iron citrate and no enthalpy change was observed[12]. Whether the iron was in the Fe(II) or Fe(III) form in this experiment is unclear, and stoichiometric amounts of Ca(II) were used. The current work indicates that >20 equiv of Ca(II) are required to fully convert CP into its high-Fe(II) affinity form, in agreement with prior observations for the high-affinity Mn(II) complex[11]. Moreover, when considering metal-binding equilibrium, the counter ion introduces another variable. Although our current work indicates that CP will outcompete citrate for Fe(II) (citrate $K_{d,Fe(II)} \sim 10^{-8}$ M) (ref. 38), citrate will affect the metal speciation in solution. Importantly, ferrous iron is susceptible to oxidation and strict anaerobic or reducing conditions are needed to maintain this oxidation state over the course of an experiment. These caveats illustrate the complexity of this system and the multiple experimental considerations that must be taken into account when studying metal-protein interactions as well as the factors that come into play when working with a redox-active metal like iron.

Our report of iron sequestration by CP may be considered from multiple perspectives. From the standpoint of metal-binding motifs found in nature, the histidine-rich site of CP is the first example of a biological Fe(II)-binding His_6 site and thereby expands the biological coordination chemistry of iron-containing proteins. Because Fe(II) is labile and undergoes rapid ligand exchange, the His_6 coordination motif provides a remarkable mechanism for sequestering Fe(II). On the basis of available binding constants, the Fe(II) affinity of CP far exceeds that of characterized proteins that include *E. coli* Fur and superoxide dismutase[30,39,40]. Thus, the molecular basis for how CP overcomes the inherent lability of Fe(II) and achieves such tight binding warrants further exploration. Guided by recent crystallographic[12,15] and spectroscopic[15] studies of Mn(II) coordination by CP at site 2, we propose that the C-terminal tail region of S100A9 encapsulates Fe(II) in this site and excludes water molecules from the vicinity of the metal center. Moreover, we anticipate that site 2 will chelate Fe(II) in a nearly idealized octahedral geometry with coordination by the Nε atoms of each histidine residue, as observed for Mn(II)[12,15]. Small-molecule Fe(II)–hexaimidazole complexes have been structurally characterized[41,42], and these coordination complexes may provide helpful benchmarks in further studies of Fe(II)-CP.

Our metal depletion studies indicate that CP also chelates copper and nickel, as expected from the Irving-Williams series. Thus, a role for CP in the homeostasis of other transition metal ions is worthy of consideration. Given the propensity of CP to chelate multiple metals (such as manganese, iron and zinc) with high affinity, the metallation and speciation of CP in the biological milieu, as well as its consequences for metal homeostasis, will depend on metal-ion availability in any given microenvironment.

From the perspective of the host-microbe interaction, iron is an essential nutrient for almost all microbes, and its sequestration is an established mechanism of innate immunity[2,3]. Host-defense proteins such as lactoferrin and siderocalin interfere with microbial Fe(III) acquisition[43,44]. To the best of our knowledge, a comparable mechanism to prevent microbial Fe(II) uptake has not previously been identified, although a number of microbes (including human pathogens) express *feoB*, a gene encoding a ferrous iron transporter, when colonizing the host[45–48]. CP is found in a number of physiological locales, and ferrous iron is prevalent under anaerobic conditions[25]. We propose that CP is a heretofore-unrecognized contributor to mammalian iron homeostasis that serves an Fe(II)-sequestering function in reducing and hypoxic microenvironments, a notion that will be addressed in future efforts.

Received 7 January 2015; accepted 1 July 2015;
published online 24 August 2015

METHODS

Methods and any associated references are available in the online version of the paper.

References

1. Bertini, I., Gray, H.B., Stiefel, E.I. & Valentine, J.S. *Biological Inorganic Chemistry: Structure and Reactivity* (University Science Books, 2007).
2. Weinberg, E.D. Nutritional immunity: host's attempt to withhold iron from microbial invaders. *J. Am. Med. Assoc.* **231**, 39–41 (1975).
3. Fischbach, M.A., Lin, H., Liu, D.R. & Walsh, C.T. How pathogenic bacteria evade mammalian sabotage in the battle for iron. *Nat. Chem. Biol.* **2**, 132–138 (2006).

4. Hood, M.I. & Skaar, E.P. Nutritional immunity: transition metals at the pathogen-host interface. *Nat. Rev. Microbiol.* **10**, 525–537 (2012).
5. Cassat, J.E. & Skaar, E.P. Iron in infection and immunity. *Cell Host Microbe* **13**, 509–519 (2013).
6. Diaz-Ochoa, V.E., Jellbauer, S., Klaus, S. & Raffatellu, M. Transition metal ions at the crossroads of mucosal immunity and microbial pathogenesis. *Front. Cell. Infect. Microbiol.* **4**, 2 (2014).
7. Sohnle, P.G., Collins-Lech, C. & Wiessner, J.H. The zinc-reversible antimicrobial activity of neutrophil lysates and abscess fluid supernatants. *J. Infect. Dis.* **164**, 137–142 (1991).
8. Corbin, B.D. *et al.* Metal chelation and inhibition of bacterial growth in tissue abscesses. *Science* **319**, 962–965 (2008).
9. Kehl-Fie, T.E. *et al.* Nutrient metal sequestration by calprotectin inhibits bacterial superoxide defense, enhancing neutrophil killing of *Staphylococcus aureus*. *Cell Host Microbe* **10**, 158–164 (2011).
10. Brophy, M.B., Hayden, J.A. & Nolan, E.M. Calcium ion gradients modulate the zinc affinity and antibacterial activity of human calprotectin. *J. Am. Chem. Soc.* **134**, 18089–18100 (2012).
11. Hayden, J.A., Brophy, M.B., Cunden, L.S. & Nolan, E.M. High-affinity manganese coordination by human calprotectin is calcium dependent and requires the histidine-rich site formed at the dimer interface. *J. Am. Chem. Soc.* **135**, 775–787 (2013).
12. Damo, S.M. *et al.* Molecular basis for manganese sequestration by calprotectin and roles in the innate immune response to invading bacterial pathogens. *Proc. Natl. Acad. Sci. USA* **110**, 3841–3846 (2013).
13. Brophy, M.B., Nakashige, T.G., Gaillard, A. & Nolan, E.M. Contributions of the S100A9 C-terminal tail to high-affinity Mn(II) chelation by the host-defense protein human calprotectin. *J. Am. Chem. Soc.* **135**, 17804–17817 (2013).
14. Vogl, T., Leukert, N., Barczyk, K., Strupat, K. & Roth, J. Biophysical characterization of S100A8 and S100A9 in the absence and presence of bivalent cations. *Biochim. Biophys. Acta* **1763**, 1298–1306 (2006).
15. Gagnon, D.M. *et al.* Manganese-binding properties of human calprotectin under conditions of high and low calcium: X-ray crystallographic and advanced electron paramagnetic resonance spectroscopic analysis. *J. Am. Chem. Soc.* **137**, 3004–3016 (2015).
16. Korndörfer, I.P., Brueckner, F. & Skerra, A. The crystal structure of the human $(S100A8/S100A9)_2$ heterotetramer, calprotectin, illustrates how conformational changes of interacting α-helices can determine specific association of two EF-hand proteins. *J. Mol. Biol.* **370**, 887–898 (2007).
17. Zaharik, M.L. & Finlay, B.B. Mn^{2+} and bacterial pathogenesis. *Front. Biosci.* **9**, 1035–1042 (2004).
18. Papp-Wallace, K.M. & Maguire, M.E. Manganese transport and the role of manganese in virulence. *Annu. Rev. Microbiol.* **60**, 187–209 (2006).
19. Jacobsen, F.E., Kazmierczak, K.M., Lisher, J.P., Winkler, M.E. & Giedroc, D.P. Interplay between manganese and zinc homeostasis in the human pathogen *Streptococcus pneumoniae*. *Metallomics* **3**, 38–41 (2011).
20. Aguirre, J.D. *et al.* A manganese-rich environment supports superoxide dismutase activity in a Lyme disease pathogen, *Borrelia burgdorferi*. *J. Biol. Chem.* **288**, 8468–8478 (2013).
21. Lisher, J.P. & Giedroc, D.P. Manganese acquisition and homeostasis at the host-pathogen interface. *Front. Cell. Infect. Microbiol.* **3**, 91 (2013).
22. Irving, H. & Williams, R.J.P. The stability of transition-metal complexes. *J. Chem. Soc.* 3192–3210 (1953).
23. Brophy, M.B. & Nolan, E.M. Manganese and microbial pathogenesis: sequestration by the mammalian immune system and utilization by microorganisms. *ACS Chem. Biol.* **10**, 641–651 (2015).
24. Archibald, F.S. & Fridovich, I. Manganese and defenses against oxygen toxicity in *Lactobacillus plantarum*. *J. Bacteriol.* **145**, 442–451 (1981).
25. Frey, P.A. & Reed, G.H. The ubiquity of iron. *ACS Chem. Biol.* **7**, 1477–1481 (2012).
26. Münck, E. in *Physical Methods in Bioinorganic Chemistry: Spectroscopy and Magnetism* (ed. Que, L., Jr.) 287–319 (University Science Books, 2000).
27. Greenwood, N.N. & Gibb, T.C. *Mössbauer Spectroscopy.* (Springer, 1971).
28. Asch, L., Adloff, J.P., Friedt, J.M. & Danon, J. Motional effects in the Mössbauer spectra of iron(II) hexammines. *Chem. Phys. Lett.* **5**, 105–108 (1970).
29. Bossek, U. *et al.* Exchange coupling in an isostructural series of face-sharing bioctahedral complexes $[LM^{II}(\mu\text{-}X)_3M^{(II)}L]BPh_4$ (M = Mn, Fe, Co, Ni, Zn; X = Cl, Br; L=1,4,7-trimethyl-1,4,7-triazacyclononane). *Inorg. Chem.* **36**, 2834–2843 (1997).
30. Cotruvo, J.A. Jr. & Stubbe, J. Metallation and mismetallation of iron and manganese proteins *in vitro* and *in vivo*: the class I ribonucleotide reductases as a case study. *Metallomics* **4**, 1020–1036 (2012).
31. Walkup, G.K., Burdette, S.C., Lippard, S.J. & Tsien, R.Y. A new cell-permeable fluorescent probe for Zn^{2+}. *J. Am. Chem. Soc.* **122**, 5644–5645 (2000).
32. Gibbs, C.R. Characterization and application of ferrozine iron reagent as a ferrous iron indicator. *Anal. Chem.* **48**, 1197–1201 (1976).
33. Stookey, L.L. Ferrozine—a new spectrophotometric reagent for iron. *Anal. Chem.* **42**, 779–781 (1970).
34. Moroz, O.V., Blagova, E.V., Wilkinson, A.J., Wilson, K.S. & Bronstein, I.B. The crystal structures of human S100A12 in apo form and in complex with zinc: new insights into S100A12 oligomerization. *J. Mol. Biol.* **391**, 536–551 (2009).
35. Brodersen, D.E., Nyborg, J. & Kjeldgaard, M. Zinc-binding site of an S100 protein revealed. Two crystal structures of Ca^{2+}-bound human psoriasin (S100A7) in the Zn^{2+}-loaded and Zn^{2+}-free states. *Biochemistry* **38**, 1695–1704 (1999).
36. Ostendorp, T., Diez, J., Heizmann, C.W. & Fritz, G. The crystal structures of human S100B in the zinc- and calcium-loaded state at three pH values reveal zinc ligand swapping. *Biochim. Biophys. Acta* **1813**, 1083–1091 (2011).
37. Liu, J.Z. *et al.* Zinc sequestration by the neutrophil protein calprotectin enhances *Salmonella* growth in the inflamed gut. *Cell Host Microbe* **11**, 227–239 (2012).
38. Königsberger, L.C., Königsberger, E., May, P.M. & Hefter, G.T. Complexation of iron(III) and iron(II) by citrate. Implications for iron speciation in blood plasma. *J. Inorg. Biochem.* **78**, 175–184 (2000).
39. Mills, S.A. & Marletta, M.A. Metal-binding characteristics and role of iron oxidation in the ferric uptake regulator from *Escherichia coli*. *Biochemistry* **44**, 13553–13559 (2005).
40. Mizuno, K., Whittaker, M.M., Bächinger, H.P. & Whittaker, J.W. Calorimetric studies on the tight binding metal interactions of *Escherichia coli* manganese superoxide dismutase. *J. Biol. Chem.* **279**, 27339–27344 (2004).
41. Carver, G., Tregenna-Piggott, P.L.W., Barra, A.-L., Neels, A. & Stride, J.A. Spectroscopic and structural characterization of the $[Fe(imidazole)_6]^{2+}$ cation. *Inorg. Chem.* **42**, 5771–5777 (2003).
42. Nistor, A., Shova, S., Cazacu, M. & Lazar, A. Hexakis(1*H*-imidazole-κN^3) iron(II) sulfate–1*H*-imidazole (1/2). *Acta Crystallogr. Sect. E Struct. Rep. Online* **67**, m1600–m1601 (2011).
43. Singh, P.K., Parsek, M.R., Greenberg, E.P. & Welsh, M.J. A component of innate immunity prevents bacterial biofilm development. *Nature* **417**, 552–555 (2002).
44. Flo, T.H. *et al.* Lipocalin 2 mediates an innate immune response to bacterial infection by sequestrating iron. *Nature* **432**, 917–921 (2004).
45. Cartron, M.L., Maddocks, S., Gillingham, P., Craven, C.J. & Andrews, S.C. Feo –transport of ferrous iron into bacteria. *Biometals* **19**, 143–157 (2006).
46. Stojiljkovic, I., Cobeljic, M. & Hantke, K. *Escherichia coli* K-12 ferrous iron–uptake mutants are impaired in their ability to colonize the mouse intestine. *FEMS Microbiol. Lett.* **108**, 111–115 (1993).
47. Konings, A.F. *et al. Pseudomonas aeruginosa* uses multiple pathways to acquire iron during chronic infection in cystic fibrosis lungs. *Infect. Immun.* **81**, 2697–2704 (2013).
48. Velayudhan, J. *et al.* Iron acquisition and virulence in *Helicobacter pylori*: a major role for FeoB, a high-affinity ferrous iron transporter. *Mol. Microbiol.* **37**, 274–286 (2000).

Acknowledgments

Research on Fe(II)-CP in the Nolan Laboratory was supported by the Office of the Director of the US National Institutes of Health (NIH grant 1DP2OD007045, E.M.N.), the MIT Center for Environmental Health Sciences (NIH P30-ES002109, E.M.N.), the Sloan Foundation and the Kinship Foundation (Searle Scholar Award, E.M.N.). T.G.N. is a recipient of the NSF Graduate Research Fellowship. Any opinion, findings and conclusions or recommendations expressed in this material are those of the author(s) and do not necessarily reflect the views of the NSF. We thank R. Laufhutte for performing the ICP-MS and ICP-OES analyses, A.J. Wommack for synthesizing ZP1 and J. Stubbe and members of her laboratory for guidance on the ^{55}Fe experiments and for providing the facilities to work with radioactivity. We acknowledge the Network on Antimicrobial Resistance in *Staphylococcus aureus* (NARSA) for providing the *S. aureus* USA300 JE2 parent strain of the Nebraska Transposon Mutant Library (NTML) that is supported by NIH NIAID grant HHSN272200700055C.

Author contributions

T.G.N. and E.M.N. designed the research. T.G.N. prepared the ICP-MS, ICP-OES and Mössbauer spectroscopy samples and conducted the microbial growth assays, ^{55}Fe uptake studies, analytical SEC, ZP1 $K_{d,Fe(II)}$ determination and metal-ion competition experiments. B.Z. and C.K. performed and analyzed the Mössbauer spectroscopy. T.G.N. and E.M.N. analyzed the results and wrote the paper.

Competing financial interests

The authors declare no competing financial interests.

Additional information

Supplementary information is available in the online version of the paper. Reprints and permissions information is available online at http://www.nature.com/reprints/index.html. Correspondence and requests for materials should be addressed to E.M.N.

ONLINE METHODS

Materials and general methods. All solvents and chemicals were obtained from commercial suppliers and used as received. All aqueous solutions were prepared using Milli-Q water (18.2 MΩ-cm, 0.22-μm filter). Buffers for metal-binding studies were prepared with Ultrol-grade HEPES (Calbiochem), TraceSELECT NaCl (Sigma) and aqueous NaOH (Sigma) in either acid-washed volumetric glassware or polypropylene containers, using Teflon-coated spatulas or polypropylene pipettes to transfer chemicals. For large-scale preparation, buffers were routinely treated with 10 g/liter Chelex resin (Bio-Rad) for at least 1 h, and the Chelex resin was subsequently removed by filtration (0.22 μm). Stock solutions of metal ions were prepared from highest-purity-available $CaCl_2$, $(NH_4)_2Fe(SO_4)_2{\cdot}6H_2O$, $FeCl_2$, $FeCl_3$ and $ZnCl_2$ (Sigma) in acid-washed volumetric glassware and were transferred to polypropylene containers. Working stock solutions of metal ions for experiments were prepared immediately before use. All experiments with Fe(II) were conducted anaerobically under a N_2 atmosphere in a Vacuum Atmospheres Company glove box unless noted otherwise, and Fe(II) solutions were prepared using the $(NH_4)_2Fe(SO_4)_2$ salt unless noted otherwise. ^{57}Fe metal powder (Isoflex) was dissolved in two-fold excess of 2 N sulfuric acid, and the concentration of the resulting $[^{57}Fe]SO_4$ solution was determined using the colorimetric ferrozine assay. Radiolabeled $[^{55}Fe]Cl_3$ was obtained from PerkinElmer as a solution dissolved in 0.5 M HCl, and experiments employing ^{55}Fe were conducted 180–210 d after the stock date. Ascorbic acid, an atomic absorption spectroscopy iron standard solution (iron(III) nitrate in nitric acid), trichloroacetic acid, ammonium acetate and ferrozine for the iron quantification assay were purchased from Sigma. Zinpyr-1 (ZP1) was synthesized from 2′,7′-dichlorofluorescein and di(2-picolyl)amine as described[31], and 2-mM stock solutions of ZP1 were prepared in DMSO, aliquoted and stored at −20 °C. All bacterial strains were stored as glycerol stocks at −80 °C. Native and mutant proteins (as well as homodimeric S100A7, S100A9^{C3S}, S100A12 and S100B) were overexpressed and purified as described elsewhere[10,11,13], and protein stocks were thawed only once immediately before use.

Antimicrobial activity (AMA) assays. The growth inhibitory activity of CP was tested by following modified literature protocols[10,13]. At least two different protein stocks and medium preparations were employed for all assays.

For evaluating the effect of Fe(II) preincubation on the antimicrobial activity of CP against *Escherichia coli* ATCC 25922 and *Staphylococcus aureus* ATCC 25923, bacterial cultures were inoculated into 5 ml TSB with 0.25% dextrose from freezer stocks or single colonies from agar plates and incubated at 37 °C on a rotating wheel. At t = 16–20 h, the overnight cultures were diluted 1:100 and incubated at 37 °C on a rotating wheel for t = 2–2.5 h until OD_{600} ~0.6 (mid-log phase). The assay medium, a 62:38 (v:v) ratio of buffer (20 mM Tris-HCl, 100 mM NaCl, 5 mM BME, 3 mM $CaCl_2$, pH 7.5) and TSB with dextrose, was prepared using sterile technique. CP samples were buffer exchanged three times into 20 mM Tris-HCl, 100 mM NaCl, pH 7.5 using presterilized 0.5-ml 10K MWCO Amicon spin concentrators, and 1.1× concentrated protein stocks (1.1 mg/mL to 68.75 μg/mL) were prepared in medium in the absence or presence of 0.9 equiv of Fe(II). The Fe(II) stock solution was prepared anaerobically and exposed to the atmosphere during the assay. The ~0.6 OD_{600} bacterial cultures were diluted 1:56 and, in a flat-bottom 96-well plate (Corning), each well was filled with 10 μl of bacterial culture and 90 μl of protein solution. Each condition was evaluated in duplicate per trial. The plates were sealed with Parafilm and incubated at 30 °C, 150 rpm. At t = 20 h, the OD_{600} values were measured using a plate reader, and the duplicate measurements were averaged for each trial. The bacterial cultures were agitated by shaking or pipetting to resuspend the cultures to homogeneity before the OD_{600} measurement. The mean OD_{600} values and s.e.m. are reported (n = 6).

For evaluating the effect of dithiothreitol (DTT) as the reducing agent in the AMA assays against *E. coli* ATCC 25922 and *S. aureus* ATCC 25923, overnight and 1:100 dilution bacterial cultures were grown as described above. The buffer for the assay medium contained 2.5 mM DTT instead of 5 mM BME. Protein samples were buffer exchanged as above, and 10× concentrated protein stocks (10 mg/ml to 625 μg/ml) were prepared in medium ± BME or DTT ± Ca(II). The ~0.6 OD_{600} bacterial cultures were diluted 1:500 into medium ± BME or DTT ± Ca(II), and 10 μl of the 10× protein stock and 90 μl of the 1:500 dilution culture were added to each well in triplicate. The plates were sealed with Parafilm and incubated at 30 °C, 150 rpm and the OD_{600} was measured at t = 20 h as described above. Three independent trials were conducted, and mean OD_{600} values and standard error are reported (n = 3).

The AMA assays against *Lactobacillus plantarum* WCFS1 were conducted as described above and employed a modified AMA medium. The medium was composed of a 62:38 (v:v) ratio of buffer (20 mM Tris-HCl, 100 mM NaCl, ± 5 mM BME, ± 3 mM Ca(II), pH 7.5) and MRS medium (CRITERION). The overnight and 1:100 dilution cultures were incubated at 30 °C, 150 rpm.

Metal analysis. Prior to the experiment, 50-ml Falcon tubes and 15-ml 10K MWCO Amicon spin concentrators were washed with 300 μM EDTA (1×) and Chelex-treated Milli-Q water (3×). The materials were then air dried and sterilized by UV irradiation (t > 15 min) before use.

AMA media ± BME ± Ca(II) were prepared using sterile technique. Protein samples were buffer exchanged into 20 mM Tris-HCl, 100 mM NaCl, pH 7.5 using 0.5-ml Amicon spin concentrators, and 2.5 ml of 10× concentrated protein stocks (1.25 or 2.5 mg/ml) were prepared using AMA media ± BME ± Ca(II). The media solutions were prepared in the washed 50-ml Falcon tubes. Untreated (0 μg/ml CP) and CP-treated (125 or 250 μg/ml) media samples were diluted to 25 ml with AMA media ± BME ± Ca(II) and incubated at 30 °C, 150 rpm. At t = 20 h, media samples were filtered in the 15-ml Amicon spin concentrators. The flowthrough samples were collected and transferred to new, washed 50-ml Falcon tubes. The tubes were sealed with Parafilm and the samples were shipped to and analyzed at the Microanalysis Laboratory at the University of Illinois at Urbana-Champaign. The concentrations of manganese, cobalt, nickel, copper and zinc were quantified by inductively coupled plasma-mass spectrometry (ICP-MS), and the metal concentrations of magnesium, calcium and iron were quantified by inductively coupled plasma-optical emission spectroscopy (ICP-OES). At least three independent preparations of media were analyzed for each sample, and analysis of the untreated media +BME ± Ca(II) was conducted during each trial as a control. The mean concentrations (μM and ppm) and the s.e.m. are reported ($n \geq 3$).

Western blot. To ensure that the CP present during treatment of growth medium did not pass through the filter, western blot analysis was employed on CP-treated medium and flowthrough samples. Sodium dodecyl sulfate-PAGE (SDS-PAGE) of the CP-Ser samples was performed on a glycine gel (15% acrylamide). The proteins were transferred to a nitrocellulose membrane following the manufacturer's procedure (BioRad). The S100A8^{C42S} and S100A9^{C3S} subunits were blotted with a 1:200 dilution of polyclonal goat IgG to human calgranulin A (sc-8112) and B (sc-8114), respectively (Santa Cruz Biotechnology). The antibodies were blotted with a 1:10,000 dilution of infrared dye–labeled donkey anti–goat IgG (LI-COR Biosciences), and the blot was visualized using a LI-COR Odyssey Scanner.

Metal-substitution bacterial growth assays. For the growth assays with *Acinetobacter baumannii* ATCC 17978, *E. coli* ATCC 25922, *E. coli* ATCC 43895 (O157:H7), *Klebsiella pneumoniae* ATCC 13883, *Pseudomonas aeruginosa* PAO1, *Bacillus cereus* ATCC 14579, *S. aureus* ATCC 25923 and *S. aureus* USA300 JE2, bacterial cultures were inoculated from freezer stocks into 5 mL TSB with dextrose and incubated overnight at 30 °C, 150 rpm (*B. cereus*) or 37 °C on a rotating wheel (all other species). At t = 16–20 h, the overnight cultures were diluted 1:100 and incubated at 30 °C, 150 rpm (*B. cereus*) or 37 °C on a rotating wheel (all other species) for t = 2–4.5 h until OD_{600} ~0.6 (mid-log phase). AMA media + BME + Ca(II) was treated with 250 μg/ml CP-Ser as described previously for the preparation of the ICP-MS samples, and the OD_{600} ~0.6 bacterial cultures were diluted 1:500 into CP-treated or untreated AMA medium. Solutions of 15 μM Mn(II), 300 μM Fe(II) and 500 μM Zn(II) were prepared and filter sterilized (0.22 μm), and 1 μl of each solution was added to each well of a 96-well plate in all possible combinations. The Fe(II) stock solution was prepared anaerobically and exposed to the atmosphere during dilution into the wells. To each of these wells, 100 μl of bacterial culture was added. The plates were sealed with Parafilm and incubated at 30 °C, 150 rpm and the OD_{600} was measured every 4 h until t = 20 h. Each condition was conducted in triplicate and the OD_{600} values were averaged per trial. Three independent trials were conducted and the mean OD_{600} values and standard error are reported (n = 3). To confirm that metal supplementation did not affect the growth of bacteria cultured in untreated medium, this procedure was conducted for the eight bacterial strains with freshly prepared AMA medium with addition of

doi:10.1038/nchembio.1891

manganese, iron, zinc or combinations thereof. Two independent trials were conducted and the means ± s.d. are reported ($n = 2$).

For the growth assays with *L. plantarum* WCFS1, the above procedure was performed with the following modifications. *L. plantarum* cultures were grown at 30 °C, 150 rpm in MRS medium. A modified AMA medium composed of Tris buffer and MRS medium (see above) was treated with 250 μg/ml CP-Ser. Bacterial cultures diluted at 1:500 were supplemented with 10 μM Mn(II) and/or 10 μM Zn(II) from filter-sterilized 1-mM M(II) stock solutions. The OD_{600} was measured at $t = 8$ h and 20 h.

^{55}Fe uptake assays. Cultures of *E. coli* ATCC 25922 and *P. aeruginosa* PAO1 from single colonies or frozen stocks were grown in a M9 minimal medium (1× M9 salts, 2 mM $MgSO_4$, 100 μM $CaCl_2$, 0.25% (w/v) glucose and 0.2% (w/v) casein) at 37 °C on a rotating wheel for 16–20 h. Overnight cultures were diluted 1:100 into 10 mL of fresh M9 medium and incubated at 37 °C on a rotating wheel until OD_{600} was ~0.6. Aliquots of cultures (1 ml) were transferred to microcentrifuge tubes and pelleted by centrifugation (3,000 rpm, 7 min, 4 °C). Cells were resuspended with 1 ml of uptake assay (UA) medium (62% (v/v) of 20 mM Tris-HCl, 100 mM NaCl, 5 mM BME, 3 mM $CaCl_2$, pH 7.5; 38% (v/v) M9 medium; supplemented with 2.7 μM $FeCl_3$ and 0.3 μM radiolabeled $^{55}FeCl_3$) with no protein, 500 μg/ml CP-Ser or 500 μg/ml ΔΔ. The cells were transferred to plastic 15-ml culture tubes, and 3 ml of UA medium with or without protein was added to each tube to obtain 4-ml cultures. The cultures were incubated at room temperature without shaking. At $t = 30$, 60, 90 and 120 min, a 500-μl aliquot of each culture was transferred to a plastic disposable cuvette to measure the OD_{600}. At each time point, 50-μl aliquots of these cultures were transferred to 0.22-μm cellulose acetate centrifuge tube filters (Corning, Inc.). The bacteria were washed with 500 μl of ice-cold wash buffer (50 mM Tris-HCl, 100 mM NaCl, pH 7.5) by centrifugation (3,000 rpm, 1 min, 4 °C) three times to remove extracellular ^{55}Fe. The washed cells were resuspended with a final 500 μl of wash buffer, and the contents of the filter were transferred to liquid scintillation vials containing 9.5 ml of Emulsifier-Safe liquid scintillation fluid. The radioactivity of the cells was measured using a Beckman LS 6500 scintillation counter averaging the counts per minute (CPM) over 3 min. The amount of bacterial ^{55}Fe uptake (reported as nmol of ^{55}Fe per mL of bacteria) was calculated using a calibration curve of CPM versus standard solutions of $^{55}FeCl_3$ (0–300 pmol). The background radioactivity of the medium and bacteria before supplementation of ^{55}Fe ($t = 0$) was also measured. The mean ± s.e.m. are reported ($n = 4$).

Analytical size-exclusion chromatography (SEC). Analytical SEC experiments were conducted on an ÄKTA purifier with a Superdex 75 10/300 GL column (GE Healthcare Life Sciences) housed at 4 °C. The calibration of the column using a low-molecular-weight calibration kit (GE Healthcare Life Sciences) and SEC elution protocol are described elsewhere[11]. Protein samples (20 μM, 300 μl) were buffer exchanged into 75 mM HEPES, 100 mM NaCl, pH 7.0 buffer before experiments. All Fe(II) samples were prepared anaerobically, sealed in microcentrifuge tubes during incubation and exposed to air immediately before injection onto the SEC column. Protein samples were loaded into a 100-μl loop and, to ensure that the total volume in the loop was transferred to the column, a 500-μl volume was injected. The protein was eluted over one column volume of running buffer (75 mM HEPES, 100 mM NaCl, pH 7.0). For samples containing Ca(II), the running buffer contained 2 mM $CaCl_2$.

Ferrozine iron quantification assay. The concentrations of iron in protein samples were determined following a modified literature protocol[49]. Standards (0 to ~60 μM Fe, 200 μl) were prepared by serial dilution in microcentrifuge tubes using an atomic absorption spectroscopy iron standard solution (iron(III) nitrate in nitric acid). To each sample, 200 μl of 1.5 mM ascorbic acid (dissolved in 0.2 M HCl) and 200 μl of 0.4 M trichloroacetic acid were added, and the resulting solution was heated to 98 °C for 10 min to denature the protein. The solutions were centrifuged to pellet the precipitate (10 min, 13,000 rpm). A 200-μl aliquot of the supernatant was transferred to a new microcentrifuge tube to which 400 μl of 1.3 M ammonium acetate and 200 μl of 6.17 mM ferrozine were added. The solutions were allowed to incubate for >5 min at room temperature, and the absorbance at 562 nm was measured.

Protein samples (400 μM, 200 μl) in the absence or presence of 5 equiv of Fe(II) or Fe(III) were prepared. The analytical SEC protocol described previously was performed on these samples, and 0.5-ml fractions were collected in polypropylene tubes. The CP concentration in each fraction was determined by absorbance ($\varepsilon_{280} = 18{,}450\ M^{-1}\ cm^{-1}$), and 200 μl of the fraction was treated and analyzed as described above. The concentration of iron in the protein samples was determined by employing a standard curve over the concentration range of 0–60 μM iron. To confirm that this protocol allows for detection of high-affinity Fe(III) binding, this experiment was performed on protein samples containing 200 μM apotransferrin (dissolved from a lyophilized powder from Sigma), 3 equiv of Na_2CO_3 (Sigma) and 3 equiv of Fe(III). Ferrozine iron analysis of the protein fractions confirmed that transferrin retained >1 equiv of Fe(III) relative to protein concentration (data not shown).

Optical absorption and fluorescence spectroscopy. Quartz cuvettes with 1-cm path lengths (Starna) were rinsed with 20% nitric acid and thoroughly washed with Milli-Q water before use. Protein samples were buffer exchanged into a 75 mM HEPES, 100 mM NaCl, pH 7.0 buffer. Optical absorption spectroscopy was performed employing a Beckman Coulter DU 800 spectrophotometer with a Peltier temperature controller. Fluorescence spectroscopy was performed employing a Photon Technologies International QuantaMaster 40 fluorometer outfitted with a continuous xenon source for excitation, autocalibrated QuadraScopic monochromators, a multimode PMT detector and a circulating water bath. The emission spectra were recorded and integrated using the FelixGX software package. Absorbance and emission spectra were measured at 25 °C.

Mössbauer spectroscopy. CP samples were buffer exchanged (75 mM HEPES, 100 mM NaCl, pH 7.0) and concentrated to ~2.3 mM. A 370-mM $CaCl_2$ stock solution was prepared and deoxygenated. A 100-mM ^{57}Fe(II) stock solution was prepared by dissolving ^{57}Fe metal in 1 M H_2SO_4 and diluting the solution with deoxygenated buffer (75 mM HEPES, 100 mM NaCl, pH 7.0). In microcentrifuge tubes inside the anaerobic glove box, 400-μl solutions of 600 μM CP, 500 μM ^{57}Fe(II) and 12 mM Ca(II) were prepared in 90% (v/v) 75 mM HEPES, 100 mM NaCl, pH 7.0 and 10% (v/v) glycerol. After 6 h of incubation under anaerobic conditions at room temperature, 300 μl of the protein solutions were transferred to Mössbauer cups. The samples were placed in an anaerobic cooling chamber chilled with liquid N_2 for 10 min for freezing. The cups housing the frozen samples were then quickly stored in insulation vials, and the filled vials were removed from the glove box and transferred to a storage dewar containing liquid N_2. The samples were stored on dry ice or at −80 °C until analysis.

Mössbauer spectra were recorded on an alternating constant acceleration Mössbauer spectrometer equipped with a Janis SVT-400 variable-temperature cryostat. The external magnetic field at the sample was oriented parallel to the γ-beam. The Mössbauer isomer shifts are referenced relative to the centroid of the spectrum of α-iron at room temperature. Simulations of Mössbauer spectra were carried out using WMOSS spectral analysis software package (http://www.wmoss.org, SEE Co., Edina, MN).

Mn(II) substitution experiment monitored by EPR spectroscopy. Continuous-wave room-temperature electron paramagnetic resonance (EPR) spectroscopy was employed to monitor the displacement of Mn(II) from CP by Fe(II). Spectra were obtained using a Bruker EMX spectrometer outfitted with an ER 4199HS cavity and a Bruker Biospin flat quartz cell. Solutions (400 μl) of either 22.5 μM $MnCl_2$ in buffer (75 mM HEPES, 100 mM NaCl, pH 7.0) or 25 μM CP-Ser, 1.25 mM $CaCl_2$ and 22.5 μM $MnCl_2$ with or without the addition of 22.5 μM $(NH_4)_2Fe(SO_4)_2$ were incubated in an anaerobic glove box at room temperature for 7 d. Each sample was removed from the glove box and immediately transferred to the flat cell. The sample was exposed to air during this time. The room-temperature EPR spectrum was recorded (20-mW microwaves at 9.83 GHz, 1.0-mT modulation amplitude). Using the software SpinCount, the free Mn(II) concentration of each sample was calculated by scaling the inner four lines of the EPR spectrum to that of a 100-μM Mn(II) solution prepared using an atomic absorption standard (Fluka) and measured under identical spectrometer conditions. Three independent trials were conducted, and the mean ± s.d. are reported ($n = 3$).

Fe(II) substitution experiment as monitored by ferrozine. Samples (1.5 ml) of 25 μM CP-Ser ΔHis_3Asp (in the absence or presence of 50 equiv of Ca(II)) were prepared in 2.0-ml microcentrifuge tubes in the glove box (75 mM HEPES, 100 mM NaCl, pH 7.0). Either Fe(II), Zn(II) or Mn(II) (0.9 equiv) was added and the mixture incubated for 30 min. A second metal ion (either 0.9 or 3.0 equiv) was added to the solution. At $t = 1$, 2, 6 and 24 h after addition of the

second metal ion, a 300-µl aliquot of the sample was removed from the glove box and immediately transferred to a 0.5-ml 10K MWCO Amicon spin concentrator (Millipore). The sample was centrifuged for 5 min (13,000 rpm, 4 °C). The protein remained in the filter, and 100 µl of the flowthrough solution, which contained unbound metal ions, was collected. A 100-µl aliquot of the flowthrough was added to 395 µl of buffer (75 mM HEPES, 100 mM NaCl, pH 7.0) and 5 µl of a 100-mM ferrozine solution (1 mM final concentration). The absorbance at 562 nm was measured after a 5-min incubation. The concentration of unbound Fe(II) was calculated using a standard curve. Additional control samples, such as CP-Ser ΔΔ incubated with Fe(II), were also measured following the same protocol. Details of each experimental condition, such as metal concentration and order of metal addition, are described in the text where relevant. Three independent trials were conducted, and the means ± s.d. are reported (n = 3).

49. Carter, P. Spectrophotometric determination of serum iron at the submicrogram level with a new reagent (ferrozine). *Anal. Biochem.* **40**, 450–458 (1971).

doi:10.1038/nchembio.1891